Supporting Information

In Situ Growth of Pd Nanoparticles on Wood for Highly Sensitive Hydrogen Sensing

Wanli Lin [a,b], Ming Li [b,c,], Zechun Li [b,c], Shaojin Shi [b,c], Changkun Zhu [b], Jun Yan [b,d], Ying Chen [b,c], Pengcheng Xu [b,c,*], and Xinxin Li [b,c,*]*

[a] College of Chemistry and Materials Science, Shanghai Normal University, Shanghai 200234, China.

[b] State Key Lab of Transducer Technology, Shanghai Institute of Microsystem and Information Technology, Chinese Academy of Sciences, Shanghai 200050, China.

[c] School of Microelectronics, University of Chinese Academy of Sciences, Beijing 100049, China.

[d] School of Opto-Electronic Engineering, Guilin University of Electronic Technology, Guilin 541004, China.

Corresponding authors

[*] Email: E-mail: liming01@mail.sim.ac.cn (M.L.); xpc@mail.sim.ac.cn (P.X.); xxli@mail.sim.ac.cn (X.L.)

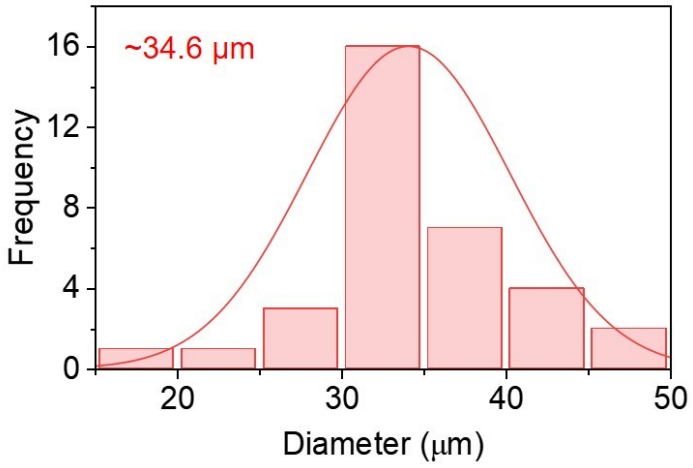

Figure S1. Diameter distribution histogram of the vertical channels in balsa wood.

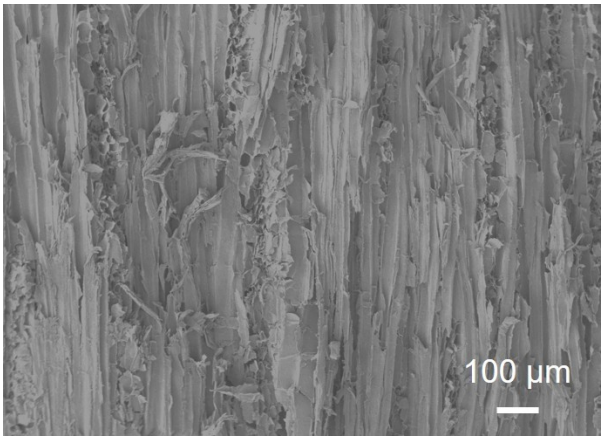

Figure S2. SEM image of the Pd NPs@Balsa sample.

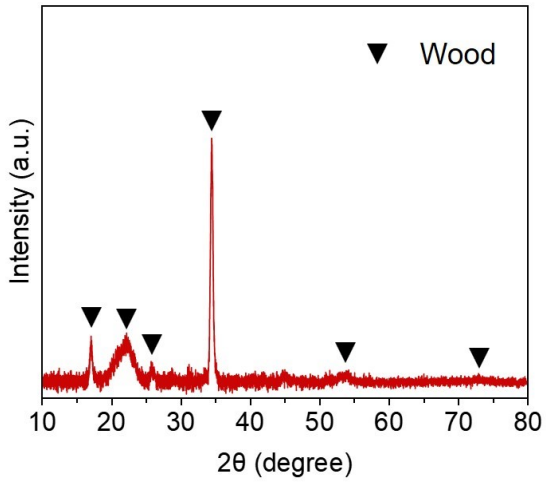

Figure S3. XRD pattern of the pristine balsa wood.

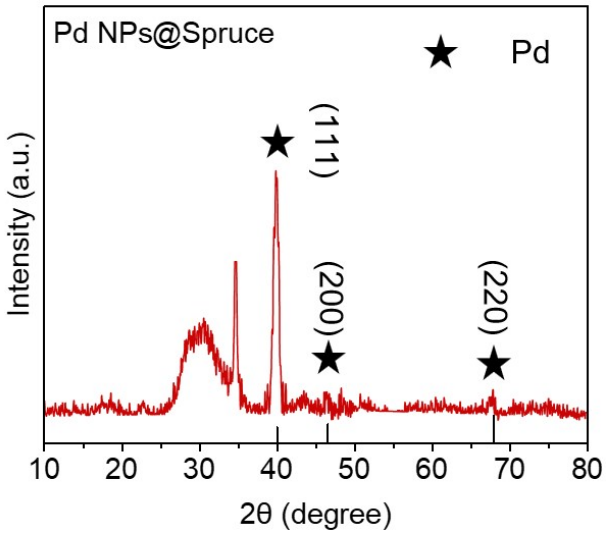

Figure S4. XRD pattern of Pd NPs@Spruce.

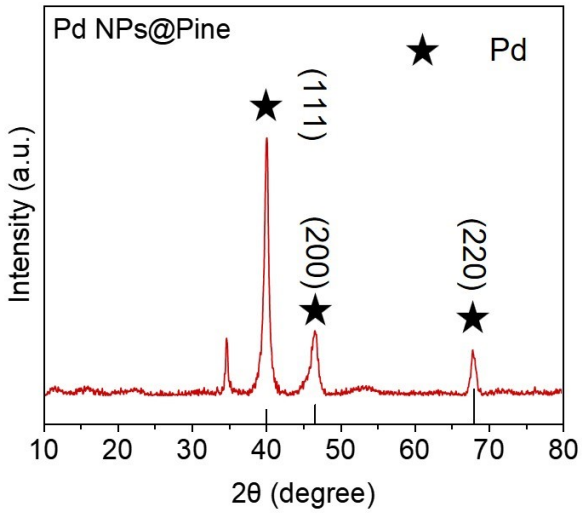

Figure S5. XRD pattern of Pd NPs@Pine.

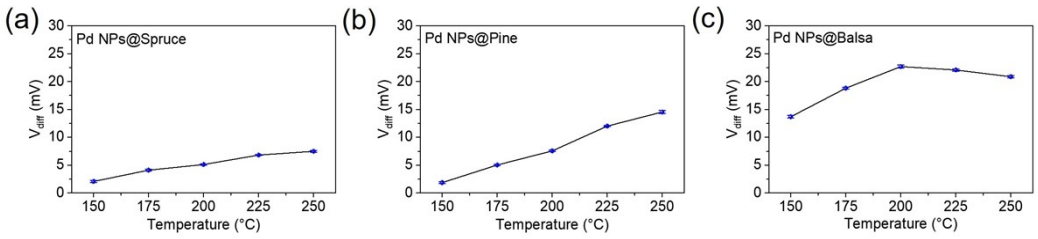

Figure S6 Comparison of the responses of three wood-based sensors to 1000 ppm H_2 at different operating temperatures: (a) Spruce, (b) Mongolian pine and (c) Balsa wood-based sensors.

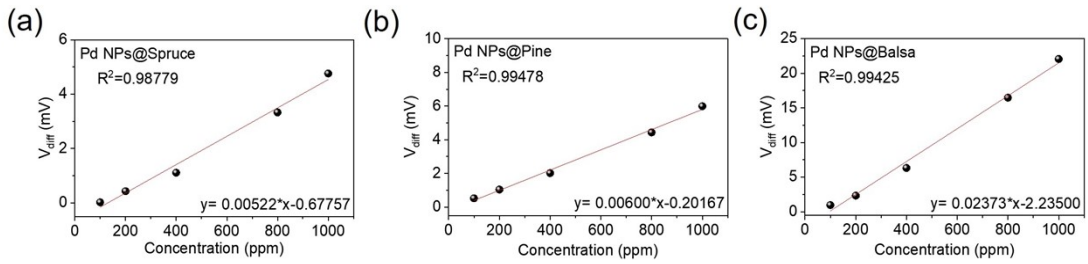

Figure S7. Calibration curves of three wood-based sensors in the H_2 concentration range of 100-1000 ppm: (a) Spruce, (b) Mongolian pine and (c) Balsa wood-based sensors.

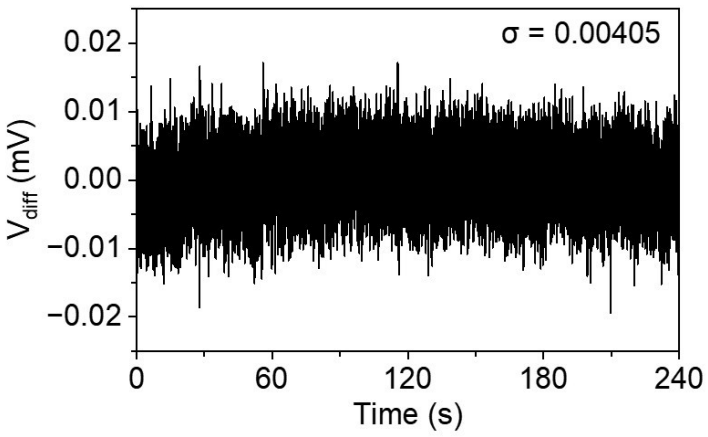

Figure S8. Magnified view of the baseline signal.

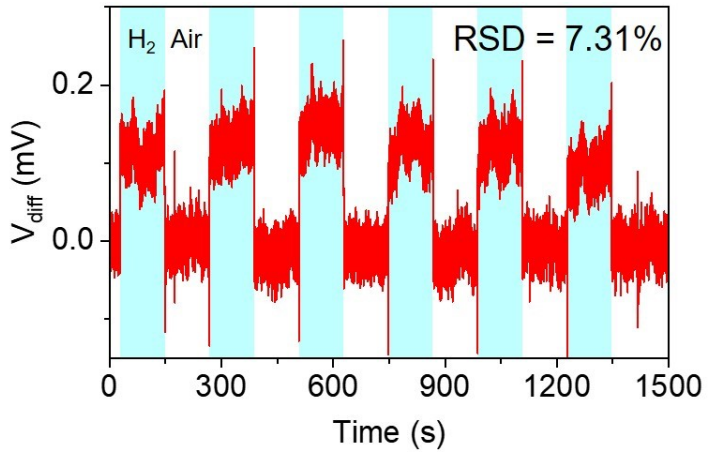

Figure S9. Repeatability test of the sensor at a low H_2 concentration of 1 ppm.

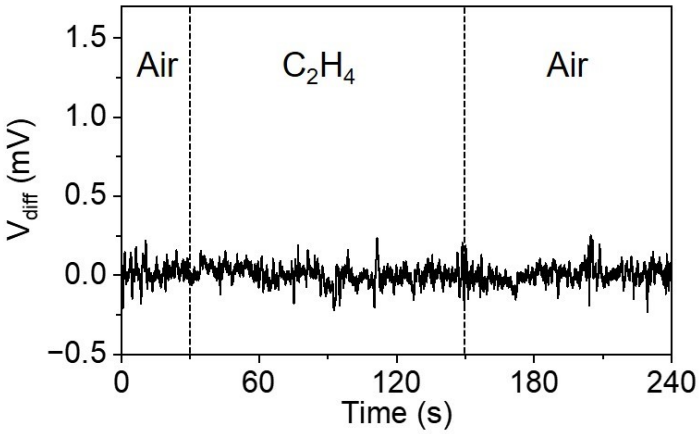

Figure S10. Response curve of the sensor to 1 ppm ethylene gas, showing no response signal.

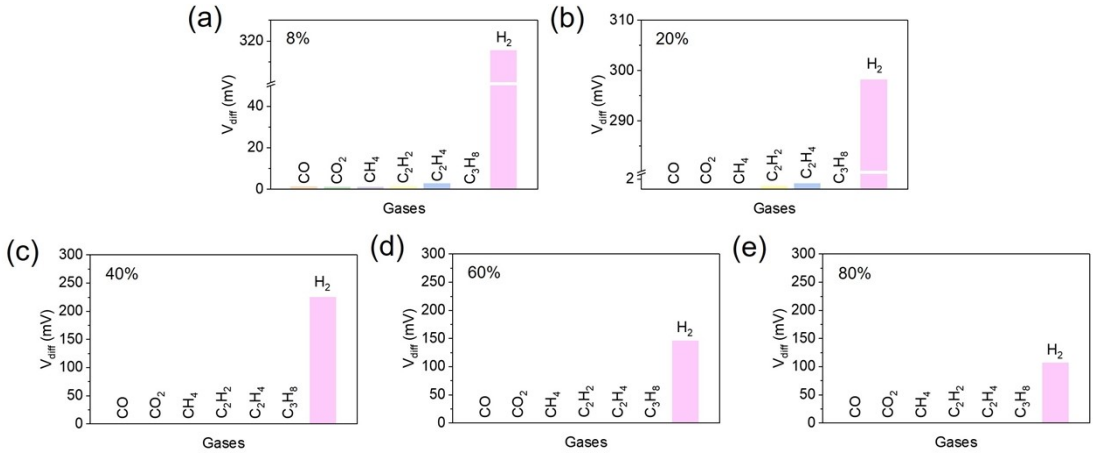

Figure S11. Comparison of sensor responses to 1% H_2 and six interfering gases under different relative humidity levels: (a) 8%, (b) 20%, (c) 40%, (d) 60%, and (e) 80%.

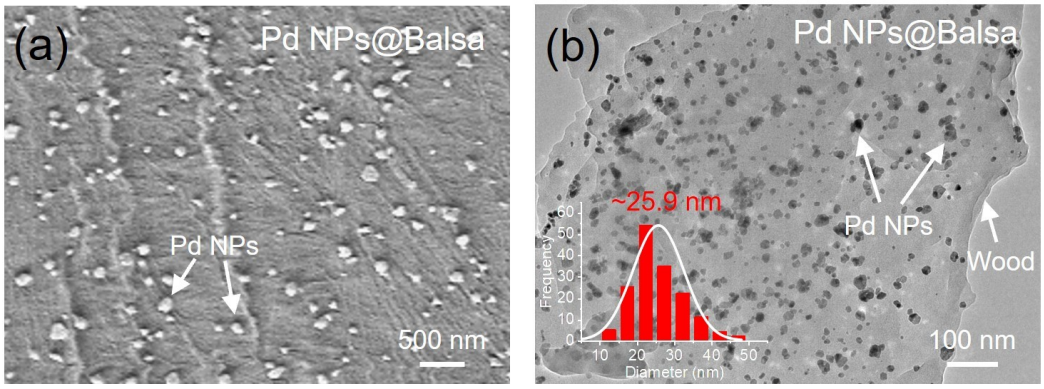

Figure S12. (a) SEM image, (b) TEM image, and particle size distribution analysis (inset in (b)) of the Pd NPs@Balsa composite after one month of stability testing.

Table S1. Comparison of the performance between this work and reported palladium-based H_2 sensors

Sensing material	Operating temp. (°C)	Detection limit (ppm)	Response time / Recovery time (s)	Ref.
Pd NPs@Balsa (MEMS)	200	1	5.4/2.5	This work
Pd-Au alloy thin film (MEMS)	60	5	22/160	S1
Polycrystalline Pd nanowires (paper-based)	RT	10	4.9/10.6	S2
Pd/SnS_2/SnO_2 nanocomposites	300	10	1/9	S3
Pd/ZnO nanorods	175	7	18/40	S4
Pd/M-WO_3	RT	1000	80/10	S5

References

[S1] J. Gong, Z. Wang, Y. Tang, J. Sun, X. Wei, Q. Zhang, G. Tian and H. Wang, Journal of Alloys and Compounds, 2023, 930, 167398.

[S2] A. Kumar, K. Chen, T. Thundat and M. T. Swihart, ACS Applied Materials & Interfaces, 2023, 15, 5439-5448.

[S3] X. Meng, M. Bi, Q. Xiao and W. Gao, Sensors and Actuators B: Chemical, 2022, 359, 131612.

[S4] S. Kumar, S. D. Lawaniya, S. R. Nelamarri, M. Kumar, P. K. Dwivedi, Y.-T. Yu, Y. K. Mishra and K. Awasthi, Sensors and Actuators B: Chemical, 2023, 394, 134394.

[S5] C.-H. Wu, Z. Zhu, S.-Y. Huang and R.-J. Wu, Journal of Alloys and Compounds, 2019, 776, 965-973.